

Numerical Analysis of the Sea State Bias for Satellite Altimetry

R. Glazman, A. Fabrikant

Jet Propulsion Laboratory, California Institute of Technology, Pasadena, CA 91109. U.S.A.

and

M.A. Srokosz

RSADU, Rennell Centre, Chilworth, Southampton SO1 7NS, United Kingdom

ABSTRACT

Theoretical understanding of the sea state bias (SSB) dependence on wind-wave conditions has been achieved only for a case of a uni-directional sea at equilibrium with a steady wind [Jackson, 1979; Glazman and Srokosz, JPO, 21 (11), 1991]. Recent analysis of Geosat and Topex altimeter data showed that additional factors, such as the presence of swell, ocean currents and complex directional properties of realistic wave fields, may influence the SSB behaviour [Glazman et rd., 1994]. Here we investigate effects of two-dimensional multi-modal wave spectra using a numerical model of radar reflection from a random, non-Gaussian surface. A recently proposed ocean wave spectrum is employed to describe sea surface statistics. The following findings appear to be of particular interest: 1) Sea swell has an appreciable effect in reducing the SSB coefficient compared to the pure wind sea case, but less effect on the actual SSB due to the corresponding increase in significant wave height, 2) Hidden multi-modal structure (that is, when the two-dimensional wavenumber spectrum contains separate peaks - for swell and wind seas, while the frequency spectrum looks uni-modal) results in an appreciable. change of SSB. 3) For uni-mods], purely wind-driven seas, the influence of the angular spectral width is relatively unimportant, that is, a uni-directional sea provides a good qualitative model for SSB if the swell is absent. 4) The pseudo wave age is generally much better for parameterising SSB than the actual wave age (which is ill-defined for a multi-modal sea). 5) SSB can be as high as five percent of the significant wave height, which is significantly greater than predicted by present empirical model functions. 6) Parameterisation of SSB in terms of wind speed is likely to lead to errors, due to the dependence on the (in practice, unknown) fetch.

August 1994

1. introduction

The present work pursues two goals: one is to construct a mathematical model of the wave field relevant to open ocean conditions, and the other - more practical - is to develop an "experimental" tool for the investigation of altimeter response to various factors of air-sea interaction. This study addresses rather complex physical processes: spatial evolution of a statistically anisotropic field of sea surface roughness caused by wind-driven waves and swell, and the nadir backscatter of a short radar pulse from a non-Gaussian random surface. The second issue is of considerable practical importance in connection with satellite altimeter measurements of ocean surface topography.

The sea state bias (SSB) correction remains among major limiting factors of altimeter measuring accuracy. Currently, SSB is estimated based on wind speed and significant wave height (SWH) information available from altimeter measurements. Under idealised sea conditions (as discussed in section 2), wind and SWH are, indeed, sufficient - they permit derivation of SSB employing some empirical relationships. Since the wind speed and SWH are the only parameters of air-sea interaction available from altimeter measurements, this simple-minded approach is extremely attractive. In general, wind and SWH are of course insufficient to describe a sea state and estimate SSB [Glazman et al., 1994]. In order to understand the limitations of the present empirical approach and identify other important parameters, experimental and theoretical studies are necessary.

In section 4 we evaluate the relative importance of additional characteristics of sea state - which cannot be derived from altimeter measurements. These are sea swell arriving from remote ocean areas and variations in the angular width of wave spectra. The latter can be caused by interaction of surface waves with ocean currents or by variations in wind direction, and so on. These factors received little attention in the previous studies. This effort is partly motivated by the need to understand causes of recent 1 y reported regional anomalies in the SSB regime [Glazman et al., 1994].

We employ the geometrical optics theory [Brown, 1977; Barrick and Lipa, 1985; Jackson, 1979; Srokosz, 1986, 1987] which relates two main components of SSB to sea surface parameters (that is, to the surface skewness and mean height of specular wave facets) and a semi-empirical model for wind sea spectra [Glazman, 1993, 1994] appropriate for open ocean conditions. This model is complemented

with a spectral model of swell. Diffraction effects due to small-scale ripples, considered earlier by Rodriguez. et al. [1992], are outside the scope of the present work. These effects may become important for a detailed analysis of dual-frequency altimeters, such as Topex. The main difference between the present work and the preceding studies by Jackson [1979] and Glazman and Srokosz [1991] is that we now implement the full two-dimensional version of the theory [Srokosz, 1986] which uses angular wave spectra and allows investigation of complex wave systems. Additionally, we avoid certain simplifications made earlier. Particularly, we include both SSB components - the surface, skewness component, λ_0 , and the specular height component, λ_1 . The former was neglected by Glazman and Srokosz [1991] on the grounds that its contribution is appreciably smaller at large wave age values, at least for unidirectional wave spectra. The theoretical model is described in section 3, the numerical results are summarised in section 4, and the conclusion of the study presented in section 5.

2. Spectral model of sea surface roughness

Field measurements [Glazman and Pilorz, 1990; Glazman, 1993, 1994] show that under open ocean conditions, wave spectra tend to be much broader than those measured in lakes or closed or semi-closed sea basins, such as bays, internal seas and coastal regions. The spectral width increases with an increasing wind as well as with an increasing degree of wave development characterised by the wave age and wind fetch. In order to cover a broad range of sea states, we use here, for the wind-driven component of the wave field, a recently developed semi-empirical spectrum model [Glazman and Srokosz, 1991; Glazman, 1993; 1994]. The angular spread function $\Psi(\Theta/\Theta_0)$ is chosen in an analytical form that permits studying effects of the angular width of the spectrum. An adjustable parameter Θ_0 represents the characteristic angular width of the spectrum. The wind-driven component of our two-dimensional spectral model is given by the following set of relationships:

$$F(k, \Theta) = \beta(U^2/g)^{2\mu} k^{-4+2\mu} \exp[-(k/k_0)^2] \Psi'(\Theta/\Theta_0) \exp[-(kh)^2], \quad (2.1)$$

The wave age ξ is defined as the ratio of the phase velocity of spectral peak waves to the mean wind speed, U (at 10 m height). β is a “generalised Phillips constant.” Its dependence on the wave age (alternatively, on the non-dimensional wind fetch) is determined (empirically as well as theoretically) for the range of ξ from 1 to 3 [Glazman, 1993,1994]. At the values of ξ typical to open ocean conditions ($\xi \geq 1.5$), β varies rather little, and for most practical purposes it can be taken as $\beta \approx 1.7 \cdot 10^{-3}$. Its empirically-based dependence on the wave age is given by

$$\beta \approx (1.51 + 2.15 \xi^{-3.15}) \cdot 10^{-3} \quad (2.2)$$

which represents a fit to the open ocean data reported earlier [Glazman, 1994]. Furthermore, g is the acceleration of gravity, k_0 is the spectral peak wavenumber related to the wave age, ξ , by

$$k_0 = (g/U^2)\xi^{-2} \quad (2.3)$$

μ is a function of the wave age, which can be interpreted as a fractal index of the surface. Based on the field data [Glazman, 1994], this function is “approximated as:

$$\mu \approx 0.633 - 0.638 \xi^{-1.13} \quad (2.4)$$

Finally, h is the inner scale of the gravity-wave spectrum which serves as a low-pass filter smoothing out small-scale ripples whose dynamics and statistics are governed by mechanisms different from those implied in (2.1) [Glazman and Weichman, 1989; Glazman and Srokosz, 1991; Glazman, 1993]. For sufficiently small values of ξ , such that $\mu(\xi) \rightarrow 0$, (2.1) approaches the Pierson-Moskowitz spectrum, while at moderate degrees of sea development, the “inertial” range of (2.1) takes the form of the Zakharov-Filonenko spectrum (see also, Donelan and Pierson [1987]). The wave age ξ can be expressed as a function of the nondimensional wind fetch using either theoretical expressions or empirical relationships (summarised, for example, in Glazman [1994]). For simplicity, we shall present our numerical results as a function of ξ and $\delta_0 (= k_0 h)$.

To investigate the role of the angular width of the spectrum, we choose the angular spread function in a simple form

$$\Psi(\Theta/\Theta_0) = A_{wnd}(\Theta_0) \exp \left[-(\Theta/\Theta_0)^2 \right], \quad (2.5)$$

where normalisation constant A_{wnd} is given by

$$A_{wnd}^{-1} = \int_{-\pi}^{\pi} \exp\left[-(\Theta / \Theta_0)^2\right] d\Theta = \sqrt{\pi} \Theta_0 \quad (2.6)$$

Although this form is rather simple, it appears to capture most of the significant effects of angular spread on SSB. We have experimented with a variety of forms (including wavenumber dependent angular spread functions) and found that more complicated forms yield practically the same end results as @.5- (2.6). It should be noted that equation (2.6) is an approximate result (strictly the result requires integration from $-\infty$ to ∞), but for the small values of @ used here it is perfectly adequate.

The second component of the wave spectrum is due to swell and is specified in the form:

$$F_{swl}(k, @) = A_{swl} \exp\left(-[(\Theta - \Theta_{swl}) / \Delta\Theta_{swl}]^2\right) \exp\left(-[(k - k_{swl}) / \Delta k_{swl}]^2\right) \quad (2.7)$$

where normalisation constant A_{swl} is

$$A_{swl} = \frac{a_{swl}}{\pi \Delta\Theta_{swl} \Delta k_{swl}} \quad (2.8)$$

where a similar approximation to that used in calculating A_{wnd} above has been made.

The parameters Δk_{swl} and $\Delta\Theta_{swl}$ provide measures of spectral width, a_{swl} is the swell amplitude (squared). The full wave spectrum is obtained as the sum of (2. 1) and (2.7). Illustrations for two specific sets of parameters, studied later in the paper, are provided in Figure 6.

In altimeter-based studies, where direct information on the actual wave age is not available, a pseudo wave age has proved useful. This quantity is defined as

$$\xi_p = A(gH / U^2)^{2v} \quad (2.9)$$

where A and v are empirical parameters (in general, they are not constant) whose approximate values and dependence on external factors of air-sea interaction can be derived based on wave dynamics theory [Glazman, 1993; 1994]. Following the previous empirical estimates, we use here $A = 3.24$ and $v = 0.31$. As shown in section 4, this measure of the sea maturity may have a closer relation to the sea state

bias in a mixed sea than does the actual wave age. The latter can be unambiguously defined only for a uni-modal wave system. With the model used here it is, of course, possible to calculate, both the wave age (of the wind sea component) and the pseudo wave age directly and, if desired, examine their behaviour.

3. The two-dimensional model of the sea state bias

Based on the work by Longuet-Higgins [1963], Srokosz [1986] derived a two-dimensional version of the geometrical optics theory for the sea state bias (SS13). The end-point result is

$$SSB = -\frac{1}{8}\left(\frac{\lambda_0}{3} + \lambda_1\right)H_{1/3}, \text{ or } SSB = -\epsilon H_{1/3} \quad (3.1)$$

where $H_{1/3}$ is the significant wave height obtained from the full spectrum as

$$H_{1/3}^2 = 16 \int_0^{\infty} k dk \int_{-\pi}^{\pi} F(k, \Theta) d\Theta \quad (3.2)$$

The expression for the surface skewness, λ_0 , is given in terms of the two-dimensional wavenumber spectrum by Srokosz [1986], and is not much different from its one-dimensional counterpart employed in [Glazman and Srokosz, 1991]. The expression for the mean relative height of the specular points is provided below (with a few insignificant corrections made to the originally published relationship):

$$\lambda_1 = \frac{\lambda_{120} + \lambda_{102} - 2\lambda_{011}\lambda_{111}}{1 - \lambda_{011}^2} \quad (3.3)$$

where

$$\lambda_{120} = \frac{\int_0^{\infty} \int_{-\pi}^{\pi} F(k) \left[\int_0^{\infty} \int_{-\pi}^{\pi} F(k') \left([k^2 \cos^2 \Theta + (k')^2 \cos^2 \Theta'] C(k, k') - k \cos \Theta k' \cos \Theta' S(k, k') \right) dk' \right] dk}{\left[\int F(k) dk \right]^{1/2} \int_0^{\infty} \int_{-\pi}^{\pi} k^2 \cos^2 \Theta F(k) d\Theta dk} \quad (3.4)$$

$$\lambda_{102} = \frac{\int_0^\infty \int_{-\pi}^\pi F(\mathbf{k}) \left[\int_0^\infty \int_{-\pi}^\pi F(\mathbf{k}') \left([k^2 \sin^2 \Theta + (k')^2 \sin^2 \Theta'] C(\mathbf{k}, \mathbf{k}') - k \sin \Theta k' \sin \Theta' S(\mathbf{k}, \mathbf{k}') \right) d\mathbf{k}' \right] d\mathbf{k}}{\left[\int_0^\infty \int_{-\pi}^\pi F(\mathbf{k}) d\mathbf{k} \right]^{1/2} \left[\int_0^\infty \int_{-\pi}^\pi k^2 \sin^2 \Theta F(\mathbf{k}) d\Theta dk \right]^{1/2}} \quad (3.5)$$

$$\lambda_{111} = \frac{\int_0^\infty \int_{-\pi}^\pi F(\mathbf{k}) \left[\int_0^\infty \int_{-\pi}^\pi F(\mathbf{k}') \left([k^2 \cos \Theta \sin \Theta + (k')^2 \sin \Theta' \cos \Theta'] C(\mathbf{k}, \mathbf{k}') - k \cos \Theta k' \sin \Theta' S(\mathbf{k}, \mathbf{k}') \right) d\mathbf{k}' \right] d\mathbf{k}}{\left[\int_0^\infty \int_{-\pi}^\pi F(\mathbf{k}) d\mathbf{k} \right]^{1/2} \left[\int_0^\infty \int_{-\pi}^\pi k^2 \sin^2 \Theta F(\mathbf{k}) d\Theta dk \right]^{1/2} \left[\int_0^\infty \int_{-\pi}^\pi k^2 \cos^2 \Theta F(\mathbf{k}) d\Theta dk \right]^{1/2}} \quad (3.6)$$

$$\lambda_{011} = \frac{\int_0^\infty \int_{-\pi}^\pi F(\mathbf{k}) k^2 \sin \Theta \cos \Theta dk}{\left[\int_0^\infty \int_{-\pi}^\pi k^2 \sin^2 \Theta F(\mathbf{k}) d\Theta dk \right]^{1/2} \left[\int_0^\infty \int_{-\pi}^\pi k^2 \cos^2 \Theta F(\mathbf{k}) d\Theta dk \right]^{1/2}} \quad (3.7)$$

where

$$C(k, k') = (kk')^{-1/2} [B^-(k, k') + B^+(k, k') - \mathbf{k} \cdot \mathbf{k}' + (k + k')(kk')^{1/2}] \quad (3.8)$$

$$S(k, k') = (kk')^{-1/2} [B^-(k, k') - B^+(k, k') - kk'] \quad (3.9)$$

$$B^\pm(k, k') = \frac{(\sqrt{k} \pm \sqrt{k'})^2 (\mathbf{k} \cdot \mathbf{k}' \mp kk')}{(\sqrt{k} \pm \sqrt{k'})^2 - |\mathbf{k} \pm \mathbf{k}'|} \quad (3.10)$$

For a one-dimensional surface considered earlier [Glazman and Srokosz, 1991], many of the components making up (3.1) have been expressed in a relatively simple analytical form which allows one to better understand the impact of wind-wave parameters on these components, the present case requires a numerical solution. Employing the full spectrum described in section 2, the integration was carried out using some of the routines in the IMSL and NAG Fortran libraries. The double integrals in

(3.2) and (3.4)-(3.6) were calculated with the relative precision of 0.01. The results are presented in the next section.

4. Results and discussion

Due to the complexity of numerically evaluating four dimensional integrals (see equations 3.3 to 3.10) and because of the number of adjustable parameters that **are** involved in the model spectra (equations 2.1 to 2.8) it is not feasible to explore the **behaviour** of the **SSB** across the full parameter space. **Therefore**, we have chosen to examine a number of specific cases to illustrate the differences from the earlier **uni-directional** spectral model of **Glazman & Srokosz** [1991], and to try to gain insight into how **SSB** behaves as a function of the parameters (specifically the significant wave height $H_{1/3}$ and the wind speed U) that an altimeter can measure.

4.1 Comparison with the results of Glazman & Srokosz [1991]

We begin our presentation of results by comparing the numerical calculations of this paper with the analytical results of **Glazman & Srokosz** [1991; denoted **GS hereafter**] for the case of a **uni-directional** spectrum. The two studies are **different** in three major ways: (i) the final results reported in GS used only the specular height component, λ_1 , of the total **SSB**; (ii) the model wave spectrum **employed** by GS used highly **idealised, theoretically-based** relationships for the Phillips constant and μ as functions of the wave age; (iii) the present model spectrum is two-dimensional.

Figure 1 illustrates the **SSB coefficient, ϵ** , as calculated based on the model wave spectrum presented in section 2. With the angular width $\Theta_0 = 0.1$ and inner scale $\delta_0 = 0.05$, accounting for λ_0 results in an increase of ϵ by about 10 percent (the curve **labelled old** is based on only the λ_1 term). This is consistent with the analytical results of GS (see their **Figure 4**) and the consequent neglect of the term λ_0 , as compared to λ_1 , in **their** analysis. The use of the **two-dimensional** model spectrum leads to an increase of λ_1 as **compared** to that of GS (see their **Figure 6**) by up to 50 **percent**.

To further compare the present model to GS, we provide **Figure 2** (analogous to **Figure 6** of GS) which illustrates the dependence of ϵ on the actual wave age ξ for wind driven sea with a relatively

narrow directional spread ($\Theta_0 = 0.1$). While the qualitative trends for all values of Θ_0 remain essentially the same, the magnitude of the SSB coefficient is now increased by up to 80 percent. This indicates that the simpler GS uni-directional model can lead to significant underestimation of SSB.

4.2 Behaviour of the bias as a function of measurable parameters

Using the values of Θ_0 from Figure 2, we plot SSB (3.1) in nondimensional form in Figure 3, using an intrinsic scaling based on U and g . The nondimensional form, denoted by B in Figure 3, is related to the actual SSB by $SSB = -B U^2 / g$. This intrinsic scaling may have some advantages over the form given in equation (3.1) when empirical model functions are being devised, as it has monotonic behaviour with wave age (compare Figures 2 and 3).

Practical determination of SSB is based on the pseudo wave age, which can be determined from the altimeter measurements of $H_{1/3}$ and U . Hence, it is interesting to compare the results in Figure 2 with a similar plot based on the pseudo wave age given in Figure 4. This comparison shows that the general behaviour is preserved, and calculations for a range of values of Θ_0 ($= 0.05-0.4$) give similar results. This suggests that pseudo wave age (as given by equation 2.9) might be used to parameterise SSB.

Since the presently accepted functional form of ϵ for Topex (due to E. Walsh) is given as $\epsilon(U)$ [Callahan, 1993], it is interesting to compare the empirical results for $\epsilon(U)$ with the theoretical predictions of the present model. To this end, we estimated wave model parameters, β and μ , as functions of wave age. The latter was related to the non-dimensional fetch $\tilde{x} = gX/U^2$ by

$$\xi = C\tilde{x}^c$$

where $C = 0.08$ and $c = 0.25$, as given in Table 1 of Glazman [1994]. The results are shown in Figure 5 for several values of the fetch X . Comparing this to the empirical results of Glazman et al. [1994; Figure 3] shows that the theory presented here goes some way to explaining the observations, given that the theoretical curves are calculated for fixed values of the fetch, while the empirical ones are based on observations which cover a range of wind fetch values.

4.3 Effect of the angular width of the wave spectrum on SSB

Calculating SSB as a function of external factors for the case of a **wind-driven** sea we found that SSB doesn't depend on the angular width, Θ_0 . No appreciable changes in the values of ϵ have been found as Θ_0 varied between 0.05 and 0.4, a reasonable range of values of angular spread for realistic conditions. As noted above (section 2), using directional spread functions that varied with wavenumber made little difference to the results. In order to test whether extreme variations in the angular spread made any difference we used the simpler, but less realistic, spread function: $\Psi(\Theta / \Theta_0) = 1 / (2 \Theta_0)$ for $|\Theta| \leq \Theta_0$ and $\Psi(\Theta / \Theta_0) = 0$ otherwise. Varying Θ_0 from 0.1 to 0.4 (the isotropic sea case; that is, the wavefield being statistically identical in all directions), leads to variations in ϵ of less than 15%, and for the range 0.1 to 0.4 there is less than a 2% change in ϵ across the whole range of wave age. Thus we conclude that, for wavefields characterised by a realistic angular spread, SSB is practically independent of the angular spread.

4.4 Effect of sea swell on SSB

As stated earlier in this section, the range of possible combinations of parameters that describe the effect of the interaction of wind sea and swell on SSB is too great to be fully explored. In any case, it is not our intention in this paper to try to characterise all possible situations that might arise in practice (the model spectra used are probably too simple for that). Rather, the intention is to indicate the importance of wind sea and swell interactions for SSB. Therefore, only two cases have been considered: when the typical wavelength of swell is greater than that of wind-driven seas and the opposite case. The wind-driven sea is characterised by the following parameters: $\xi=1$, $\Theta_0=0.1$, and $\delta_0=0.1$. The direction of swell propagation, Θ_{swl} , is fixed for both long-wave and short-wave swell at $2\pi/3$ with respect to the mean wind direction (that is, swell opposing wind waves).

For the "long-wave" case, the swell amplitude, a_{swl} , is 0.8β where β is the Phillips constant for wind-driven seas. The swell characteristic wavenumber, k_{swl} , is taken to be $0.25k_0$ in equation (2.3). The spectral width of the swell system, Δk_{swl} , is taken as $0.2k_0$, with the angular width $\Delta\Theta_{swl}=0.8$. For "short-wave" case: $a_{swl} = 0.2\beta$, $\Delta\Theta_{swl} = 0.33$, $k_{swl}=1.2k_0$, and $\Delta k_{swl}=0.4k_0$. To a degree

these choices are somewhat arbitrary, but nevertheless serve to illustrate the effects of wind sea and swell interactions.

The composite spectra are illustrated in Figures 6a and 6b - for the long- and short-wave swell, respectively. The bi-modal structure of the spectra can be seen clearly. While the frequency (or the wavenumber modulus) spectrum corresponding to Figure 6a also reveals the hi-modal structure of this mixed sea, this is not the case for short-wave swell of Figure 6b. As shown in Figure 7, the one-dimensional spectrum (Q variation integrated out) of this mixed sea appears as if it were uni-modal.

It is perhaps worth noting at this point that defining the wave age when the wave spectrum is multi-modal is problematical. In contrast, the pseudo wave age remains a well defined quantity (even if its physical interpretation is less obvious) and is therefore a more stable parameter to use in parametrizing the SSB empirically (as has been done previously, for example, by Fu and Glazman [1991]).

In Figures 8a and 8b, we illustrate the SSB coefficient ϵ as a function of the pseudo wave age. The SSB coefficient, ϵ , calculated for purely wind-driven seas is noticeably greater (by some 20 to 25 percent) at lower values of the pseudo wave age than that which includes swell effect, and this is the case for both the long- and short-wave swell. However, this does not translate into the SSB itself being appreciably reduced due to the swell. SSB is a product of ϵ and $H^{1/3}$, and the latter, given by equation (3.2), increases in the presence of swell. Thus, the effect of swell on the values of the SSB coefficient is to reduce the latter by up to 25 percent, but the net result, illustrated in Figure 9 for the case of short-wave swell, is that swell changes SSB by 1 to 2 cm. For the long-wave swell the difference is even smaller.

In Figure 10, calculated for the case of rather young wind seas, we show the dependence of SSB on the angle of the swell propagation: the swell effect is greatest when the swell is perpendicular to the wind-sea propagation. As might be expected on physical grounds, the dependence on the SSB on the swell propagation decreases as the wave age of wind-driven waves increases.

S. Conclusions

The results presented in this paper clearly indicate that SSB is dependent on the wave spectrum in a complex way. The main conclusions of the paper are:

1. The use of simple uni-directional spectral models (such as that of Glazman & Srokosz, [1991]) can lead to the underestimation of the SSB coefficient ϵ , and therefore of the actual SSB. Nevertheless, the simpler model of Glazman & Srokosz [1991] did show the correct qualitative behaviour of SSB as a function of wave age (and pseudo wave age) and so allowed improved empirical corrections to be developed [Fu & Glazman, 1991; Glazman et al., 1994].
2. For a range of realistic values of the angular spread, for a pure wind sea spectrum, the SSB is largely unaffected by the angular spread. Using a simpler (and therefore less realistic) angular spread function we have shown that the differences in cover the whole range of angular spread, up to and including the isotropic case, are less than 15%, for all values of wave age studied.
3. The SSB, based on our directional spectrum calculations, can be as high as 5% of $H_{1/3}$, which is considerably greater than predicted by current empirical model functions [Glazman et al., 1994] based on global data sets. However, comparison of the present prediction with the empirical model functions based on (sufficiently large) regional data sets [Glazman et al., 1994] shows excellent agreement.
4. As in earlier studies [Glazman and Srokosz, 1991; Fu and Glazman, 1991], the pseudo wave age is found to be a useful parameter in characterizing SSB. The same has not been found to be true of the wind speed (another commonly used parameter). Our results (Figure 5) show that SSB, as a function of wind speed, may differ by several centimetres (up to 10 cm) depending on the value of the actual wind fetch. This suggests that parameterisations of SSB in terms of wind speed may not be an effective way to correct altimeter height data; this is confirmed by the empirical results of Glazman et al. [1994; specifically their Figure 3].
5. The presence of swell has a strong effect on the SSB coefficient ϵ , but the SSB itself is only weakly affected by the swell. The effect is greatest when the direction of swell propagation is at right angles to that of the wind sea.

Our ability ~~to obtain these~~ conclusions rests on the numerical implementation of a two dimensional model of the wave spectrum that incorporates directional spread, This provides us with a powerful tool to study the various physical factors that influence **SSB**. While this study is by no means an exhaustive application of the model, it has shown that **better modelling** can give results and insights that should improve the empirical methods currently used to correct for **SSB**. The results **could** also be used to guide laboratory and field investigations of the **problem**.

ACKNOWLEDGEMENTS

M. Srokosz is grateful to the UK Natural **Environment** Research Council for travel funding to visit the Jet Propulsion Laboratory, which allowed this paper to be completed. **This work was** performed in part at the Jet Propulsion Laboratory, California institute of '1'ethnology, under contract with the National Aeronautics and Space Administration.

REFERENCES

- Barrick, D.F. and B.J. Lipa. 1985. Analysis and interpretation of altimeter sea echo. *Advances in Geophysics*, 27, 60-99.
- Brown, G. S., 1977. The average impulse response of a rough surface and its applications. *IEEE Trans. Antennas and Propagat.*, **AP-27**, 67-74
- Callahan, P. 1993. *Topex/Poseidon GDR Users 1 handbook (Draft-2)*, JPL D-8944 Rev. A, Jet Propulsion Laboratory.
- Donelan, M.A. and W.J. Pierson, 1987. Radar scattering and equilibrium ranges in wind-generated waves with application to scatterometry. *J. Geophys. Res.*, 92 (C5), 4971-5029.
- Fu, L.-L. . . . and R.E. Glazman, 1991. The effect of the degree of wave development on the sea-state bias in radar altimeter measurements. *J. Geophys. Res.*, 96 (C1), 829-834.
- Glazman, R.E. 1993 Wave spectra of developed seas. In: "Nonlinear Waves and Weak Turbulence," N. Fitzmaurice, D. Gurarie, F. McCaughan, W.A. Woyczynski (Eds.). *The Birkhauser Series on Nonlinear PDE's*, H. Brezis (ed.), Birkhauser-Boston.
- Glazman, R.E., 1994. Surface gravity waves at equilibrium with a steady wind. *J. Geophys. Res.*, 99 (C3), 5249-5262.
- Glazman, R.E., A. Greysukh and V. Zlotnicki, 1994. Evaluating models of sea state bias in satellite altimetry. *J. Geophys. Res.*, 99 (C6), 12,581-12,591.
- Glazman, R.E. and S.H. Pilorz, 1990. Effect of sea maturity on satellite altimeter measurements. *J. Geophys. Res.*, 95 (C3), 2857-2870.
- Glazman, R. E., and M.A. Srokosz, 1991. Equilibrium wave spectrum and sea state bias in satellite altimetry. *J. Phys. Oceanogr.*, 21 (11), 1609-1621.
- Glazman R.E. and P. Weichman, 1989. Statistical geometry of a small surface patch in a developed sea. *J. Geophys. Res.*, **94**(C4), 4998-5010.
- Jackson, F. C., 1979. The reflection of impulses from a nonlinear random sea, *J. Geophys. Res.*, 84 (C8), 4939-4943.

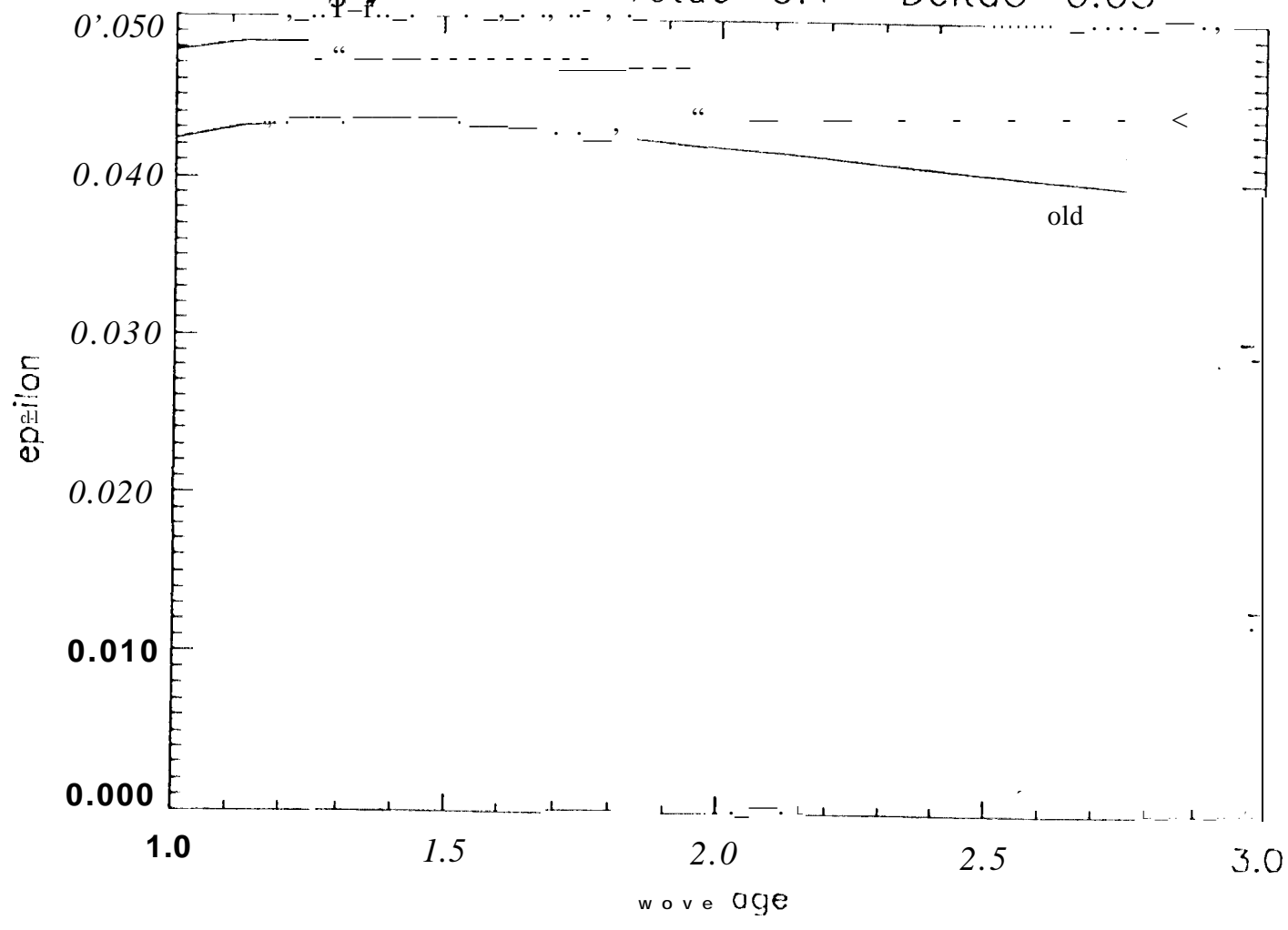
- Longuet-Higgins, M. S., 1963 The effects of nonlinearities on statistical distributions in the theory of sea waves. *J. Fluid Mech.*, **17**, 459-480.
- Rodriguez, E., 1988. Altimetry for non-Gaussian oceans: height biases and estimation of parameters. *J. Geophys. Res.*, 93 (C1 1), 14107-14120.
- Rodriguez, E., and B. Chapman, 1990. Ocean skewness and the skewness bias in altimetry: a Geosat study. *Internat. J. Rem Sens.* (To appear).
- Rodriguez, E., Y. Kim, and J.M. Martin, 1992. The effect of small-wave modulation on the electromagnetic bias. *J. Geophys. Res.*, 97 (C2), 2379-2389.
- Srokosz, M. A., 1986. On the joint distribution of surface elevation and slopes for a nonlinear random sea, with an application to radar altimetry. *J. Geophys. Res.*, 91 (C1), 995-1006.
- Srokosz., M. A., 1987. Reply to Comment by G.S.F. Lagerloef. *J. Geophys. Res.*, 92 (C3), 2989-2990.

IDL>

Fig. 7/1

Teta0=0.1

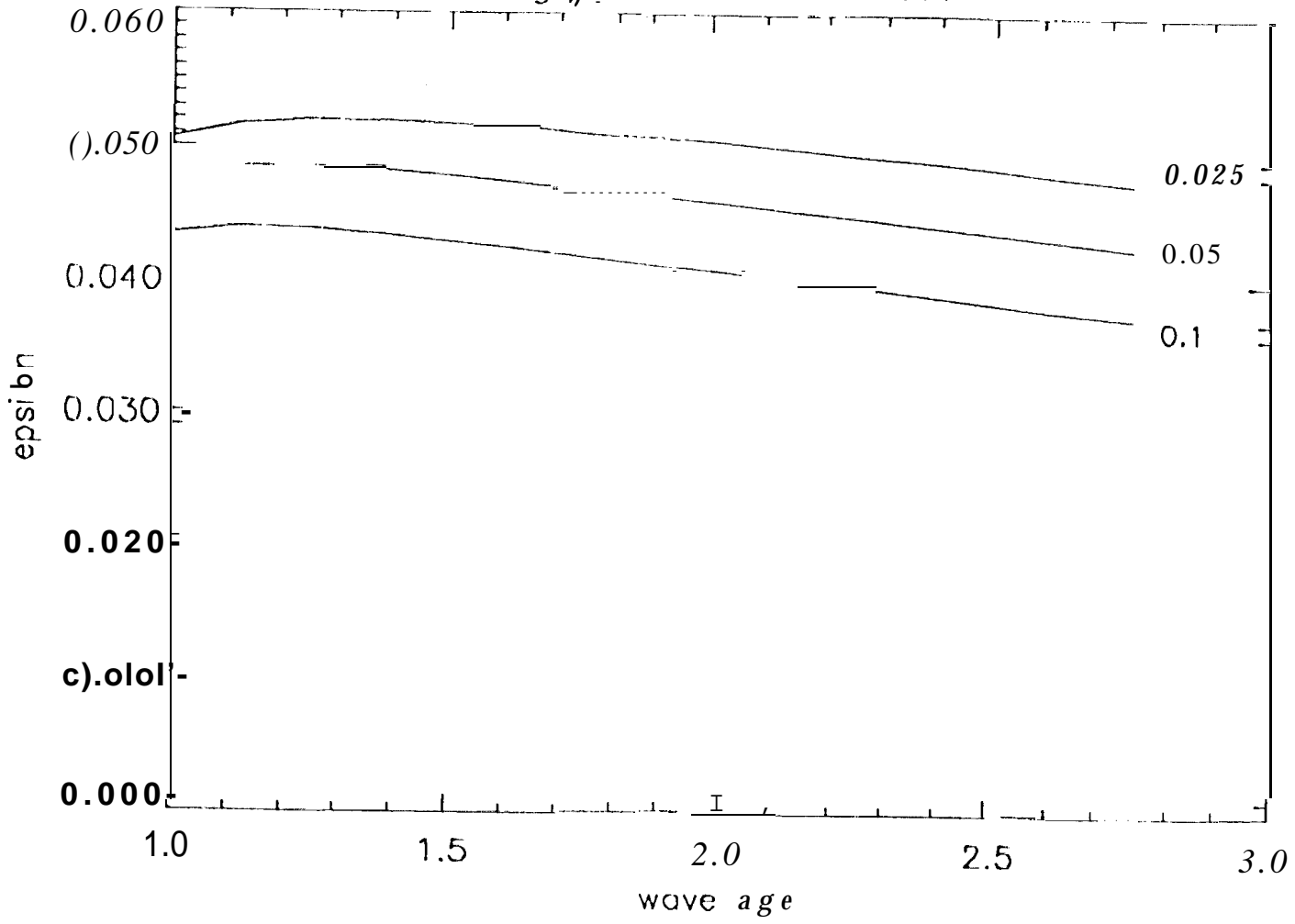
Delta0=0.05



IDL>

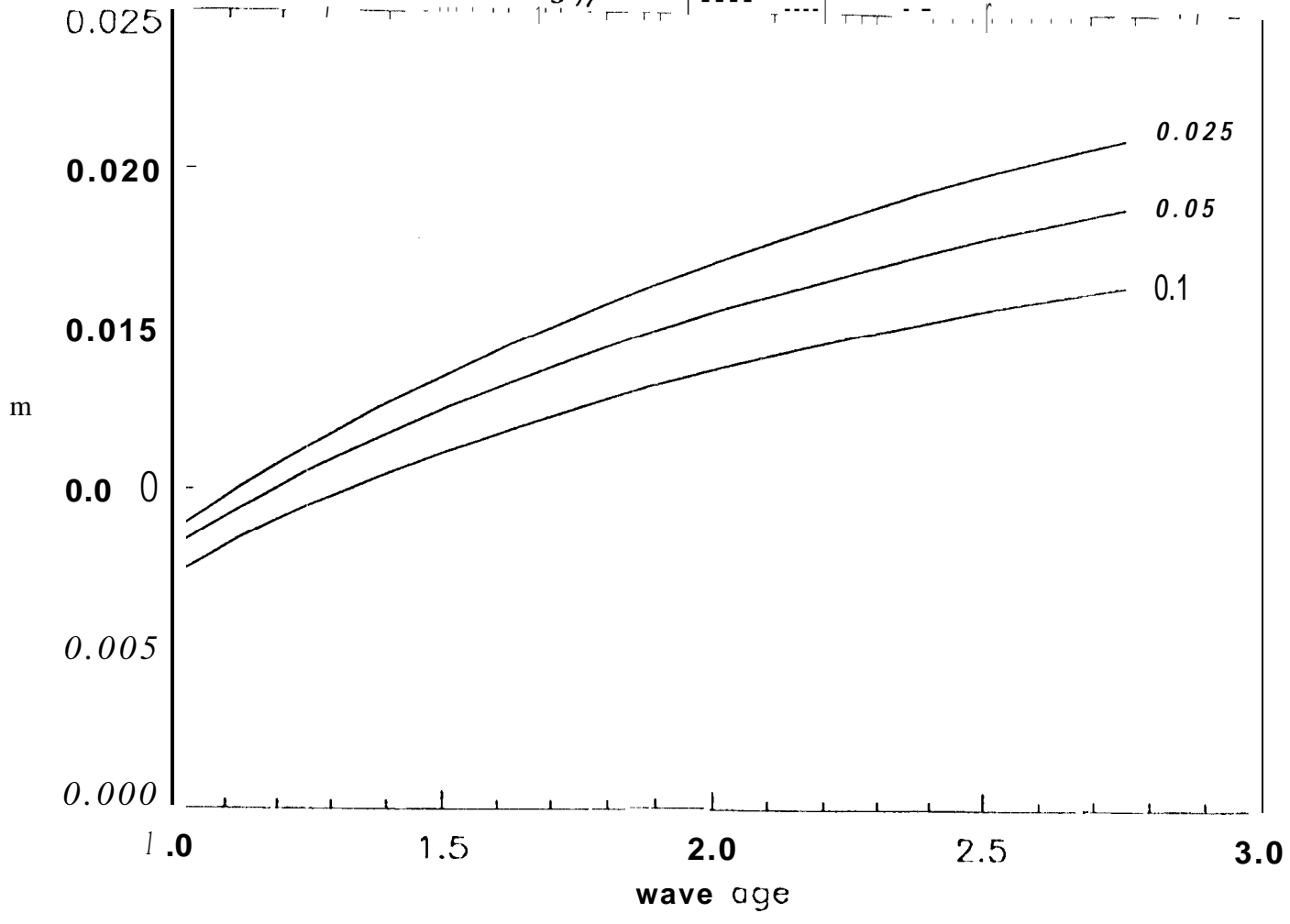
Fig. 4.2

Teta0=0.1



IDL>

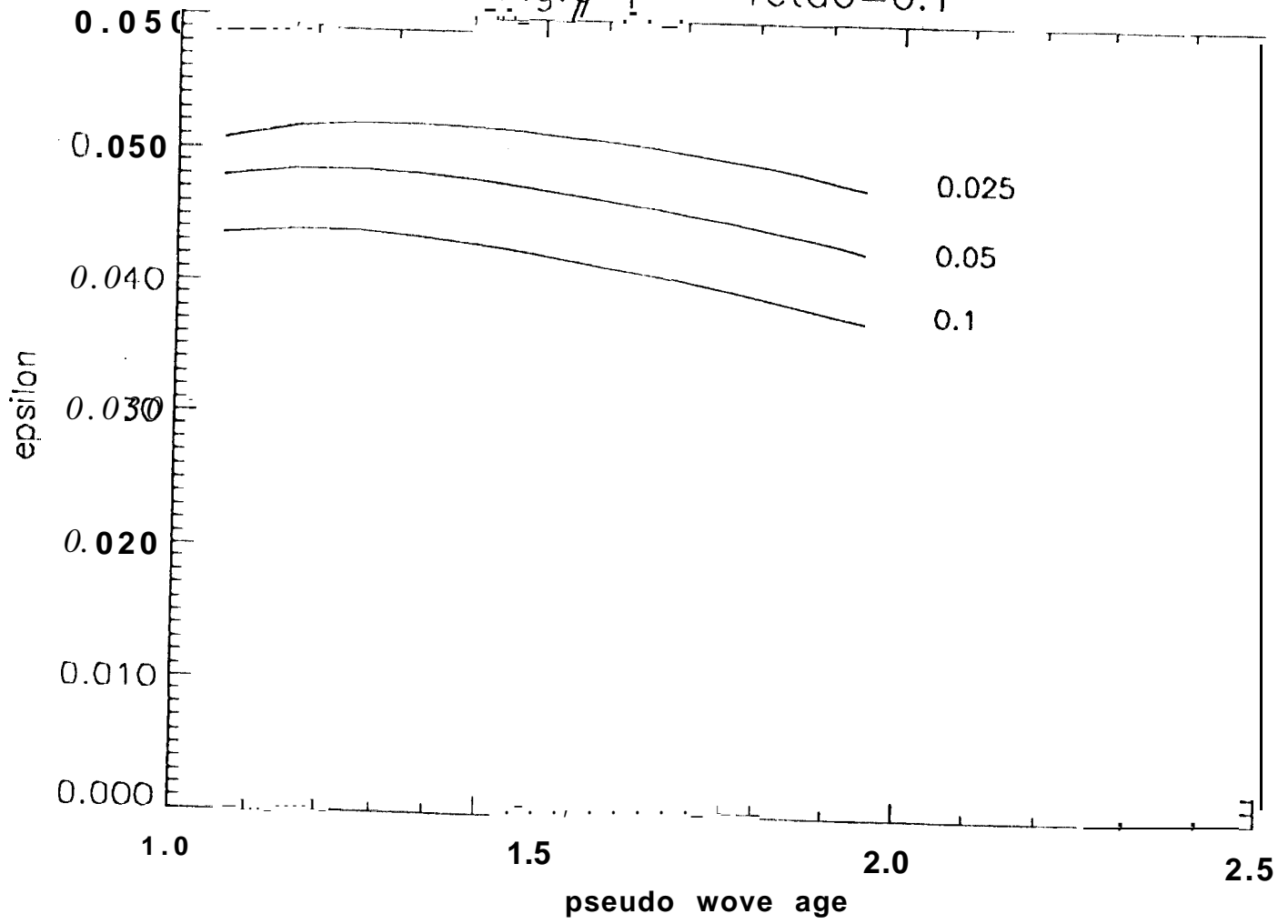
Fig. #3 $\tau_{Teta0}=0.1$



IDL>

Fig. 6/4

Teta0=0.1



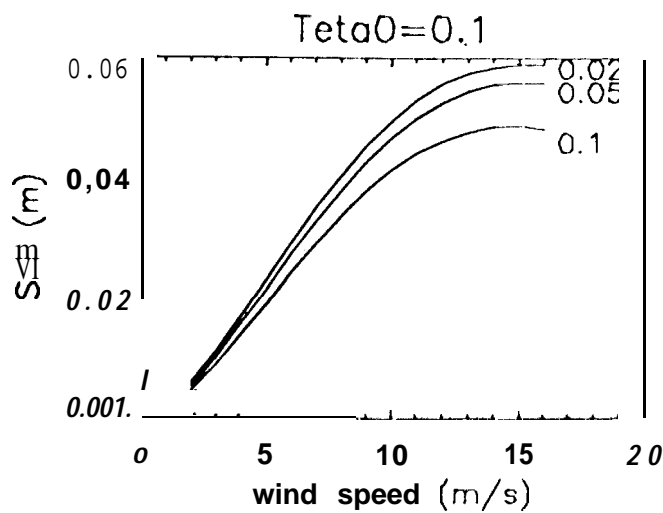
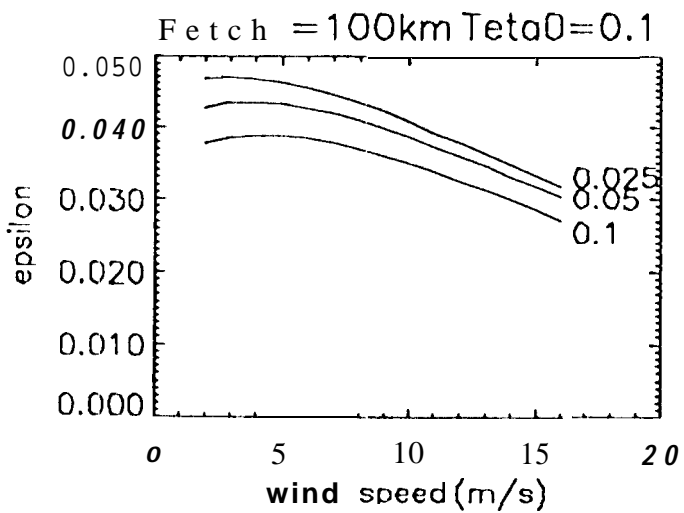
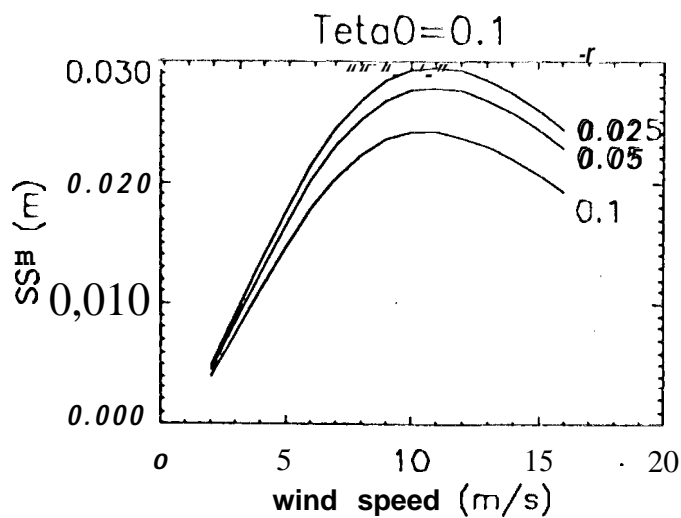
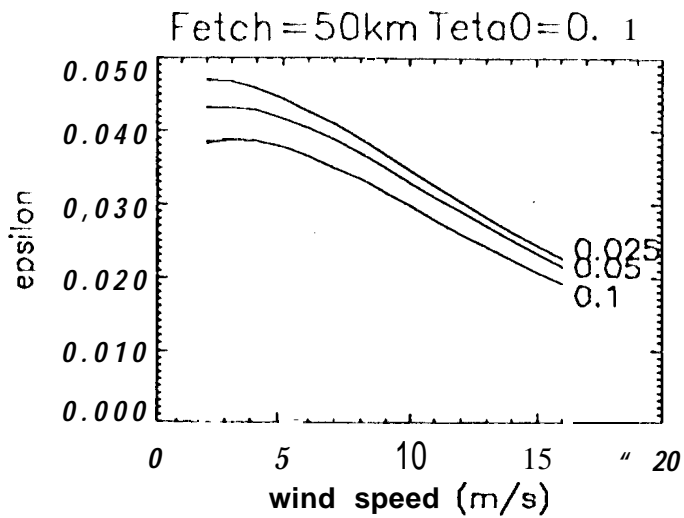
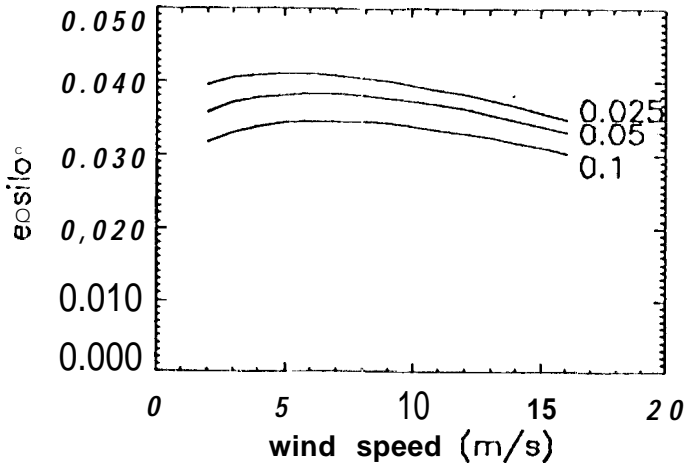


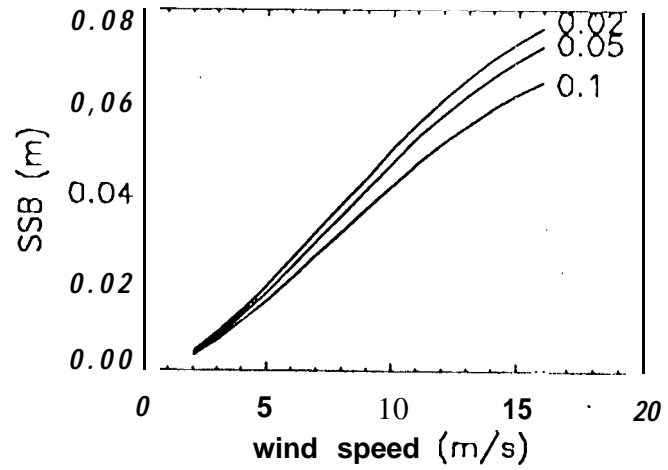
Fig. 7/ 5

IDL>

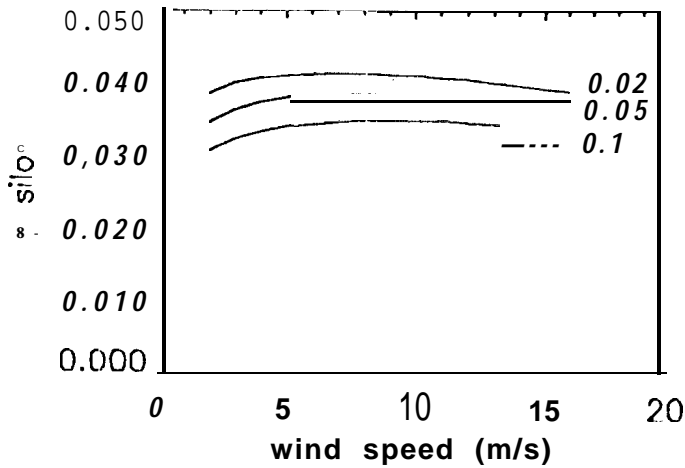
Fetch = 200km Teta0=0.1



Teta0=0.1



Fetch= 400km Teta0=0.1



Teta0=0.1

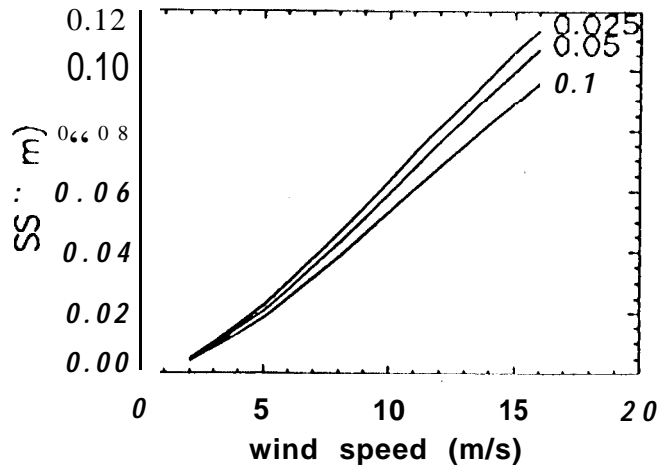
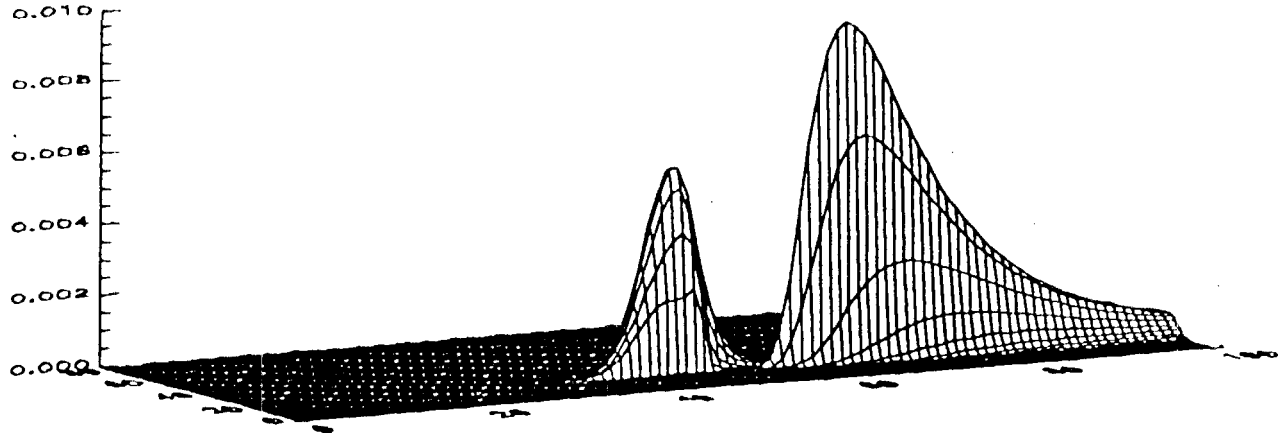


Fig. 5 (contd)

IDL >

a



b

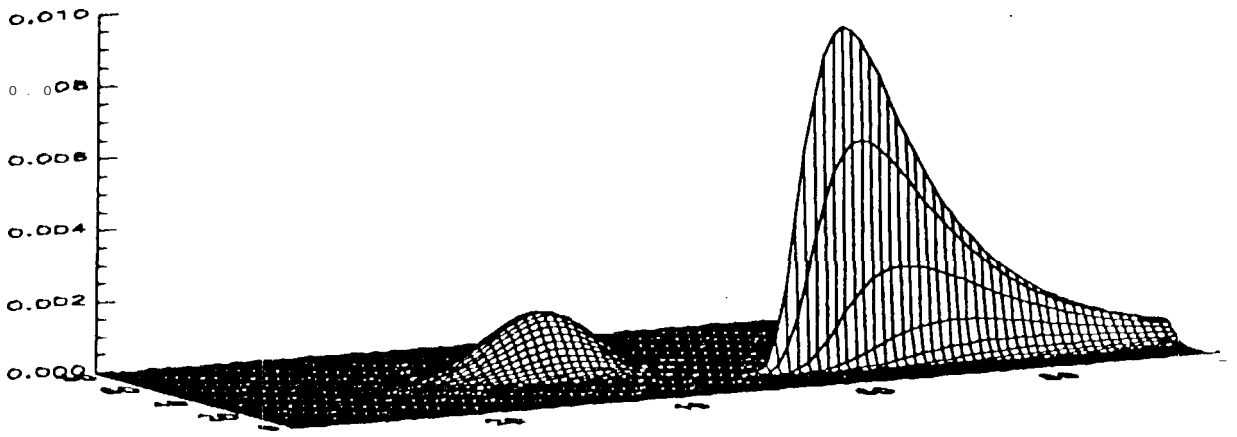


Fig. ~~6~~ 6

IDL>

Wind+ swell. $a_{sw}=0.2*b$ $k_{sw}=1.1$ $*k_0$ $k_{sw}=0.4*k_0$ $t_{sw}=2*\pi/3$

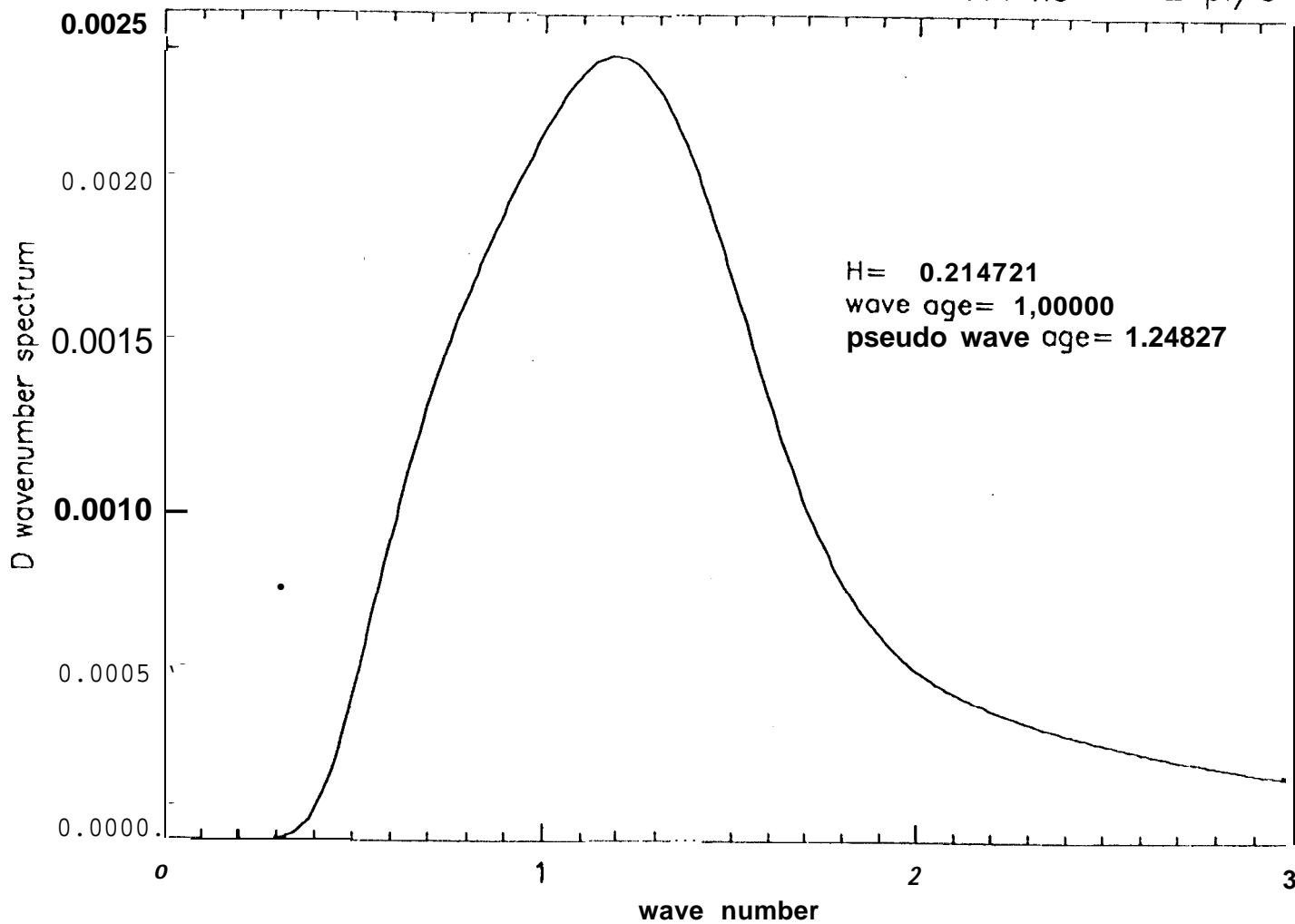
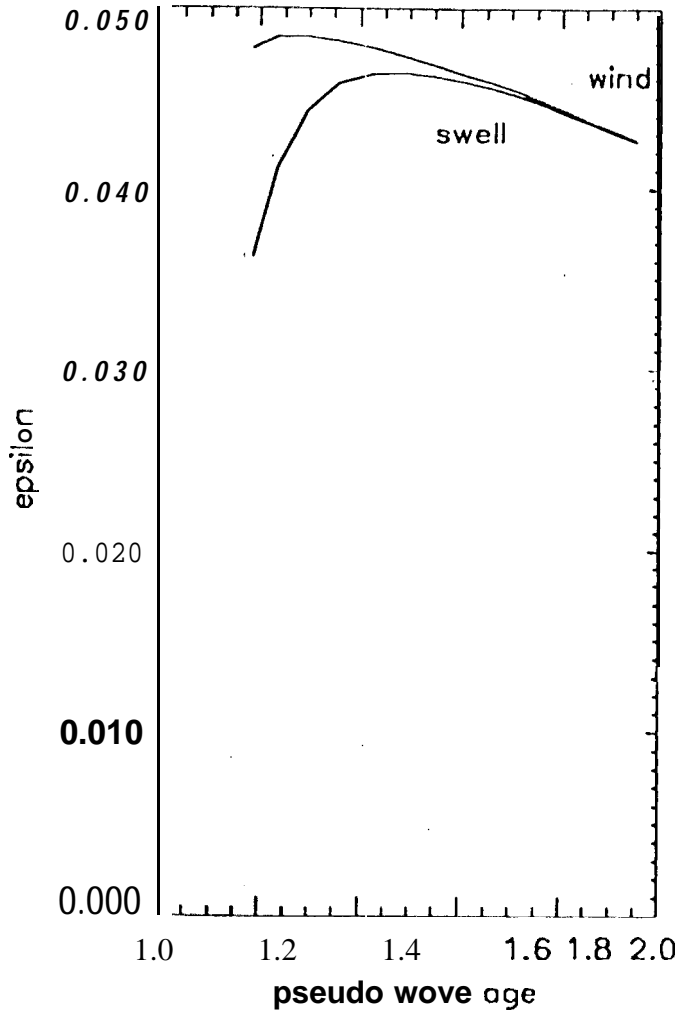


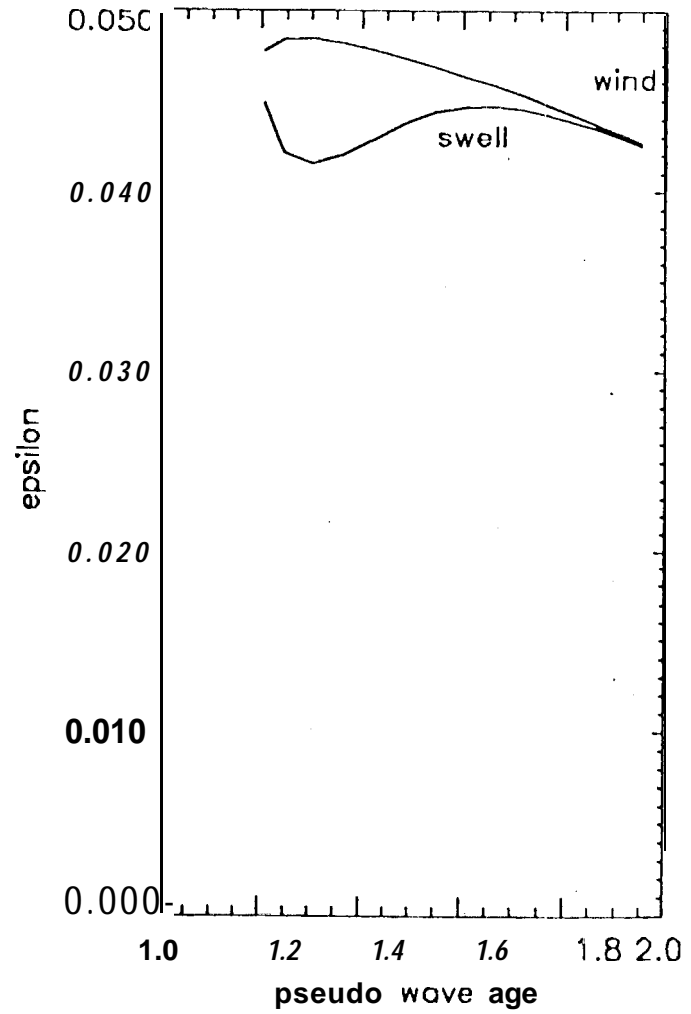
Fig. # 7

IDL> Delta=0.05 ksw=0.25*k0



a

Delta0=0.05 ksw=1.2*k0



b

Fig. ~~10~~ 8

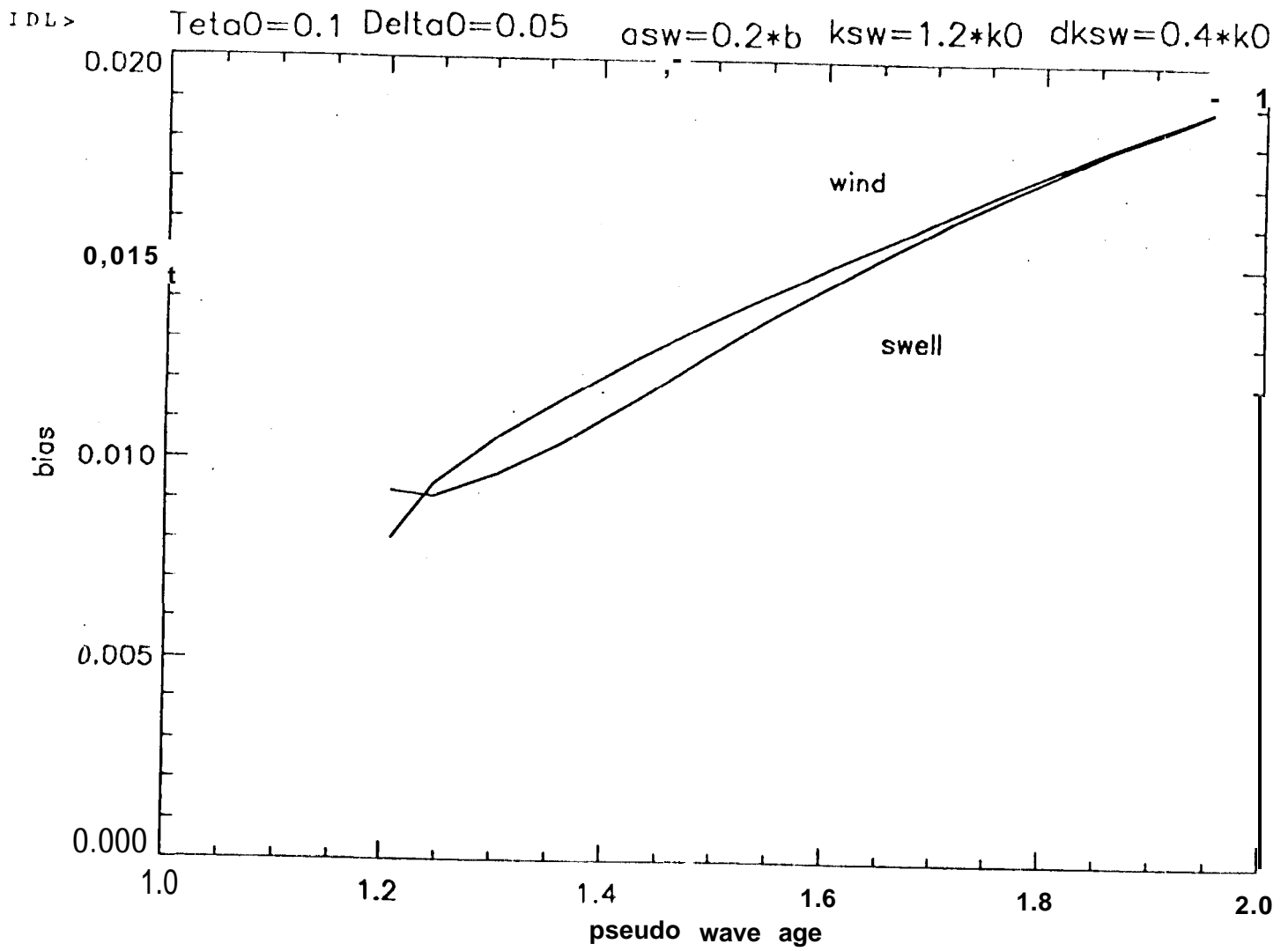


Fig. # 9

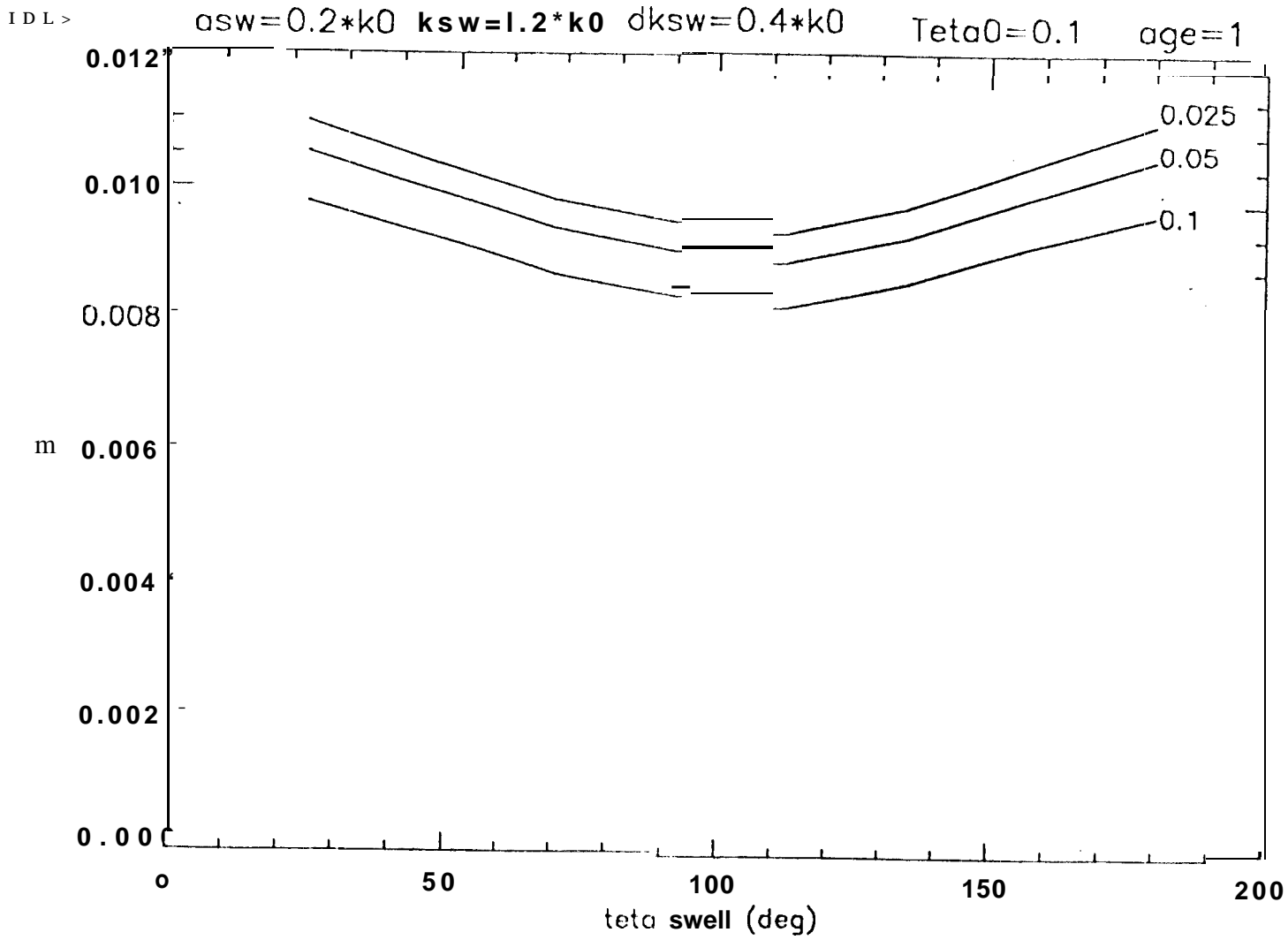


Fig. ~~10~~ 10